Monograph of Academy of Nonlinear Sciences
Advances in Nonlinear Sciences II - Sciences and Applications, Belgrade
On the application of discrete particle methods and the coupling to the continuum-based methods within a multiscale scheme 2008, Vol. 2, pp. 363-382.

ON THE APPLICATION OF DICRETE PARTICLE METHODS AND THEIR COUPLING TO THE CONTINUUM-BASED METHODS WITHIN A MULTISCALE SCHEME

Miloš Kojić

Harvard School of Public Health; University of Texas Health Science Center;
R & D Center for Bioengineering 'BioIRC' Kragujevac
665 Huntington Avenue, Building 1, Rm 1310B
Boston, MA 02115 USA
E-mail: mkojic@hsph.harvard.edu

Summary. *Several discrete particle methods are reviewed. The reviewed methods include: dissipative particle dynamics (DPD), smoothed particle hydrodynamics (SPH), element-free Galerkin and mesoscopic bridging scale (MBS) methods. The multiscale (MBS) method coupling the (DPD) and the finite element (FE) method for fluids is described, with potential future implementations. Few characteristic examples illustrate the main issues which are the subject of this presentation. A discussion about advantages and shortcomings of discrete particle methods when compared to continuum-based methods – first of all the finite element method(FEM), is presented.*

Keywords: *Dissipative particle dynamics method, smoothed particle hydrodynamics, element-free Galerkin method, multiscale mesoscopic bridging scale method.*

1 INTRODUCTION

Traditionally, continuum based methods, such as the finite element method or boundary element method, are mostly used in engineering, science and medicine**.** Their development started in the 60's of the last century. The continuous advances in the concepts, theoretical enhancements and software developments, and broadening of applications, has lead to the today's stage where these methods are used as everyday tools for modeling problems which span from simple linear analyses to multi-physics (see, e.g. [1] – [9]).

However, another group of computational methods have been emerged in last two decades. These new computational methods fall into a group of discrete particle

methods. They are developed to solve physical problems where the continuum-based methods are inappropriate, or even not applicable. For example, modeling of colloidal fluids, where a detailed analysis is required, as in case of blood flow within small blood vessels, can hardly be modeled by the FE method; or, fracture propagation in a general 3D conditions, etc. One type of these discrete particle methods relies on the approach used in molecular dynamics (MD) and we here give a brief description of the dissipative particle dynamics (DPD) method as one of the attractive and well developed methods in recent years. Another type employs the concept of discretization of physical fields in a way analogous to the FE methods (using the continuum mechanics quantities as stresses and strains), but offers advantages such as no mesh dependence or need for remeshing during the solution process. We here give a description of the two of these methods: smoothed particle hydrodynamics (SPH) and element-free Galerkin (EFG) methods.

Finally, multiscale modeling (i.e. computational models which couple the events on different space and time scales) has become the field of intensive research in last years. The multiscale methods originate from the procedures for coupling molecular dynamics and continuum mechanics representations. Along this line we here present an extension of these procedures to couple the mesoscopic DPD models and the FE models for fluids. As will be shown below, this approach can be particularly attractive for the analysis of flow of colloidal fluids where the Navier-Stokes equations may be appropriate for large domains, while a detailed DPD model is desirable in a small regions (e.g. blood flow in large arteries and thrombus development at the vessel wall).

The presentation is organized as follows. We give a brief description of the DPD method, mesocopic bridging scale (MBS) method for fluids, SPH and EFG methods. Then, few typical example solutions are presented, followed by concluding remarks in the last section.

2 DISSIPATIVE PARTICLE DYNAMICS (DPD) METHOD

2.1. Introduction to mesoscale modeling.

Molecular dynamics (MD) has been used in modeling of various processes and phenomena, particularly in chemistry, biology and medical research. However, the MD models have serious limitations since they require enormous number of equations, which are measured by billions, for even very small space domains (measured in microns) and time period. For example, in modeling of a small protein in water, half a million sets of Cartesian coordinates are generated in a nanosecond time period for the positions of 10,000 atoms [10], which is still beyond the practical capabilities of computer hardware and software currently available.

In order to overcome the limitations of the MD, the so-called coarse-graining approach has been adopted, i.e. discretization of continuum (fluids and solids) into mesoscale particles of micron length scale and micro-seconds time scale, considering these particles as clusters of atoms. This change of scales can be seen in Fig. 1 where the length and time scale domains are shown, starting from the quantum mechanics

scale to the macroscale. The mesoscale is typically in the range 10 - 1000 nm and 1 ns - 10 ms.

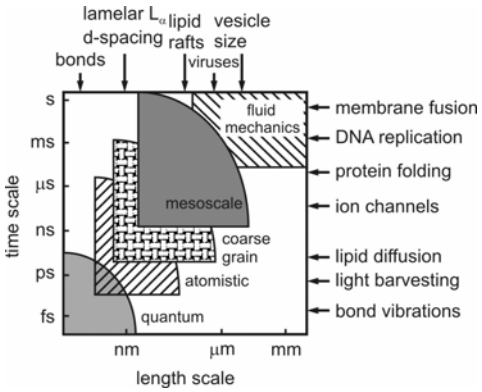

Figure 1. Models of biofluids and biosolids on various temporal and spatial scale domains [11].

The discretization into mesoscale particles is based on the Voronoi cell division (tessellation) of a continuum (e.g. [12], [13]), see Fig. 2. As in case of MD, the Lagrangian description of motion is employed, with appropriate quantification of interaction forces. One of the most developed mesoscale discrete particle methods is the dissipative particle dynamics (DPD) method, originating from work of Hoogerbrugge and Koelman [14]. The DPD method is particularly suitable for modeling polymeric and other complex fluid systems. We further summarize the basic equations of the DPD.

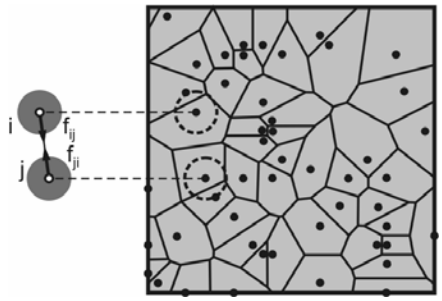

Figure 2. Discretization of space into Voronoi cells and representation of cells by mesoscopic discrete particles. The interaction forces between particles '*i*' and '*j*' are $\mathbf{f}_{ij} = -\mathbf{f}_{ji}$

2.2 Basic DPD equations

The basic equations rely on the Lagrangian description of motion. Hence, the evolution of the particle position, $\mathbf{r}_i$, can be obtained by application of the Newton second law:

$$\dot{\mathbf{r}}_i = \mathbf{v}_i$$
$$\dot{\mathbf{v}}_i = \frac{1}{m_i}\sum_{j\neq i}^{N}\hat{\mathbf{f}}_{ij} = \sum_{j\neq i}^{N}\mathbf{f}_{ij} \tag{2.1}$$

where $\mathbf{v}_i$ is the particle velocity, m_i is the particle mass; $\hat{\mathbf{f}}_{ij}$ is the force acting on particle *i* due to particle *j*, while $\mathbf{f}_{ij}$ is this force per unit mass (see Fig. 2); and the dot indicates a time derivative. The volumetric forces are neglected.

The interaction forces can be represented as the sum of three forces [15]: conservative (repulsion) $\mathbf{f}_{ij}^C$, dissipative $\mathbf{f}_{ij}^D$, and random force $\mathbf{f}_{ij}^R$:

$$\mathbf{f}_{ij} = \mathbf{f}_{ij}^C + \mathbf{f}_{ij}^D + \mathbf{f}_{ij}^R \tag{2.2}$$

These forces can expressed as:

$$\mathbf{f}_{ij}^C = a_{ij}(1-r_{ij}/r_c)\mathbf{r}_{ij}^0, \quad \mathbf{f}_{ij}^D = -\gamma w^D(\mathbf{v}_{ij}\cdot\mathbf{e}_{ij})\mathbf{r}_{ij}^0, \quad \mathbf{f}_{ij}^R = a^R w^R \xi_{ij}\mathbf{r}_{ij}^0 \tag{2.3}$$

Here, a_{ij} is the maximum repulsion force per unit mass, r_{ij} is the distance between particles *i* and *j*, $\mathbf{r}_{ij}^0 = \mathbf{r}_{ij}/r_{ij}$ is the unit vector pointing in direction from *j* to *i*, γ stands for the friction coefficient, and a^R is the amplitude of the random force. Also, w^D and w^R are weight functions for dissipative and random forces, dependent on the distance from the particle *i*; and ξ_{ij} is a random number with zero mean and unit variance. The domain of influence of the interaction forces is r_c., hence $\mathbf{f}_{ij} = \mathbf{0}$ for $r_{ij}>r_c$.

The DPD fluid system should possess a Gibbs–Boltzmann equilibrium state, hence the following relation between the weight functions of the dissipative and random forces, w_D and w_R, must hold [15].

$$w_D = w_R^2 \tag{2.4}$$

Also the amplitude of the random force a^R is related to the absolute temperature *T,*

$$a^D = \left(2k_B T\gamma\right)^{1/2} \tag{2.5}$$

where k_B is the Boltzmann constant. The weight functions can be expressed in the form [16]

$$w_D = (1-r_{ij}/r_c)^2, \quad w_R = 1-r_{ij}/r_c \tag{2.6}$$

Implementation of boundary conditions in DPD is not simple and straightforward. There are several approaches for imposing boundary conditions. For example, to impose a planar shear conditions, according to so-called Lees-Edwards method, it is assumed that the upper wall in a periodic box is moving with velocity $V_x/2$ and lower wall with-$V_x/2$. A particle crossing the upper boundary of the box at

time t is re-introduced through the lower boundary with its x-coordinate shifted by $-V_x t$ and the x-velocity decreased by V_x. For a particle crossing the lower boundary of the box, the x-coordinate shift is $V_x t$ and the x-velocity is increased by V_x. Other approaches can be found in literature, e.g. [17]-[20].

In integrating differential equations of motion (2.1) with a time step Δt, the resulting interaction force $\mathbf{f}_i$ is expressed as:

$$\mathbf{f}_i = \sum_{j \neq i} \left(\mathbf{f}_{ij}^C + \mathbf{f}_{ij}^D + \mathbf{f}_{ij}^R \left(\Delta t \right)^{-1/2} \right) \tag{2.7}$$

The coefficient $\left(\Delta t \right)^{-1/2}$ multiplying the random force comes from the integration of the stochastic equations of motion (for physical interpretation of this coefficient see [15],[16]). Various approaches has been used for the solution propagation over time, among which the so-called velocity-Verlet algorithm [16] gives the most accurate results.

3 MULTISCALE MODELING, COUPLING DPD-FE FOR FLUID FLOW

We here present a methodology of coupling the two scales for fluid flow, mesoscopic and macroscale, modeled by discrete particle DPD method (Section 2) and continuum-based FE method. This approach is called the mesoscopic bridging scale (MBS) method [21],[22]. The basic equations are given, with application on a simple example.

3.1 Introduction to multiscale modeling

A possibility to overcome limitations of the MD models is to use a multiscale approach which appropriately couples the MD and continuum methods. A review of the multiscale methods is given [23]-[26]. An extension of this multiscale approach to further couple the mesoscale and macroscale modeling is presented in this section. It relies on the bridging scale (BS) method (W. K. Liu and co-workers, see e.g. [27], [28]) of coupling MD and FE models.

The main idea of the MBS method is that the fluid velocity is decomposed into the coarse scale mean velocity and fine scale velocity fluctuation of a mesoscopic particle. The mean velocity can be calculated by a continuum-based method, such as the FE method, and the fine scale correction velocity is determined by a mesoscopic discrete particle method (e.g. DPD). Use of the appropriate projection operator provides the orthogonality of the fine scale velocities and coarse scale (FE) interpolation functions. The most significant result is that this orthogonality allows the total kinetic energy of the material system to be represented as a sum of the coarse and fine scale kinetic energies, uncoupled with respect to the velocities in the two scales. Finally, this form of the kinetic energy leads to the two systems of differential equations of motion coupled in the force terms only.

The MBS approach is particularly attractive for modeling a dilute mixture flow with a detailed insight into flow in certain local regions, as in case of, for example, blood flow in a large artery with growing thrombus at the wall caused by

adhesion of platelets. Development of the thrombus is dependent on both the global hemodynamics within the artery, and local flow and interactions between blood constituents within a small region around the thrombus. Continuum methods are applicable for modeling global artery hemodynamics, but are inadequate for determination of local flows which involve platelet activation, aggregation and adhesion.

3.2. Basic equations and boundary condition

A fluid domain is discretized into the mesoscale discrete particles, further called 'particles', representing the fine scale model; and into finite elements as the coarse scale model. One finite element is shown in Fig. 3. The basic assumption is that the velocity of a particle '*i*', $\mathbf{v}_i$, at any time, can be expressed by:

$$\mathbf{v}_i = \overline{\mathbf{v}}_i + \mathbf{v}'_i \tag{3.1}$$

where $\overline{\mathbf{v}}_i$ is the coarse scale velocity, representing the mean particle velocity, obtained by the FE method; and $\mathbf{v}'_i$ is the velocity correction, or fine scale velocity fluctuation, obtained from the fine scale solution. According to the FE method, the coarse scale velocity $\overline{\mathbf{v}}_i$ can be expressed in terms of nodal velocities, **V**, as:

$$\overline{\mathbf{v}}_i = \mathbf{N}_i \mathbf{V} \tag{3.2}$$

where $\mathbf{N}_i\left(r^i, s^i, t^i\right)$ is the matrix of interpolation functions for velocities within the finite element, with the natural coordinates of particle '*i*'; and **V** is the nodal velocity vector. The relations (3.1) and (3.2) can be written for all particles within the finite elemenl,

$$\mathbf{v} = \overline{\mathbf{v}} + \mathbf{v}' \tag{3.3}$$

$$\overline{\mathbf{v}} = \mathbf{N}\mathbf{V} \tag{3.4}$$

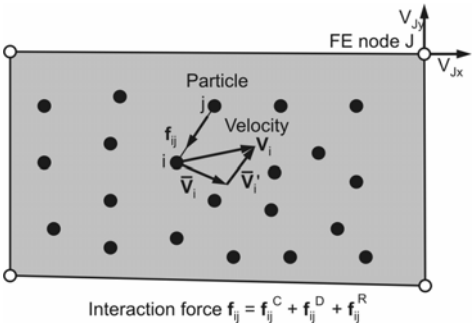

Figure 3 Discretization of fluid within a finite element into mesoscopic discrete particles; velocities and interaction forces (2D representation).

We now use a projection operator (a matrix) **Q** to express the velocity vector $\mathbf{v}'$ in terms of the nodal velocity **V**, as:

$$\mathbf{v}' = \mathbf{Q}\mathbf{v} \tag{3.5}$$

The projection operator is obtained by the minimization of a properly defined residual, so that the kinetic energy of a finite element, E_k, can be expressed as the sum of two terms, kinetic energy of the coarse (macroscale), $\overline{E}_k$, and kinetic energy of the velocity corrections from the fine scale (mesoscale), E'_k,

$$E_k = \overline{E}_k + E'_k \tag{3.6}$$

where

$$\overline{E}_k = \frac{1}{2}\overline{\mathbf{v}}^T \mathbf{M}_A \overline{\mathbf{v}} = \frac{1}{2}\mathbf{V}^T \mathbf{M}\mathbf{V} = \frac{1}{2}\mathbf{V}^T \overline{\mathbf{M}}\mathbf{V} \tag{3.7}$$

and

$$E'_k = \frac{1}{2}\mathbf{v}'^T \mathbf{M}_A \mathbf{v}' \tag{3.8}$$

Note that the terms $\overline{E}_k$ and E' are decoupled with respect to the velocities of the two scales. This decomposition of kinetic energy is the result of the fundamental importance for the MBS method for fluids.

From the principle of virtual power follow the differential equations of motion of fluid within one finite element. This mechanical system possesses $3n_a + 3N$ degrees of freedom, where n_a is the number of particles and N is the number of FE nodes (3D finite element), corresponding to particle fluctuation velocities $\mathbf{v}'$ and FE nodal velocities $\mathbf{V}$, respectively. The system is subjected to external and internal forces. The differential equations are:

$$\mathbf{M}_A \dot{\mathbf{v}}' = \mathbf{f}'^{ext} + \mathbf{f}'^{\,\mathrm{int}} \tag{3.9}$$

where $\mathbf{f}'^{ext}$ and $\mathbf{f}'^{\,\mathrm{int}}$ are the external force (such as gravity, or inertial forces due to motion of the reference coordinate system) and internal force - from action of surrounding particles, respectively; and

$$\mathbf{M}\dot{\mathbf{V}} = \mathbf{F}^{ext} + \mathbf{F}^{\mathrm{int}} \tag{3.10}$$

where the vectors $\mathbf{F}^{ext}$ and $\mathbf{F}^{\mathrm{int}}$ are the external and internal forces corresponding to the FE nodal velocity vector $\mathbf{V}$. The forces $\mathbf{f}'^{ext}$ and $\mathbf{f}'^{\,\mathrm{int}}$ can be further expressed in terms of the forces $\mathbf{f}^{ext}$ and $\mathbf{f}^{\mathrm{int}}$ acting on particles [9] as:

$$\mathbf{f}'^{ext} + \mathbf{f}'^{\,\mathrm{int}} = \mathbf{Q}^T \left(\mathbf{f}^{ext} + \mathbf{f}^{\mathrm{int}} \right) \tag{3.11}$$

The system of equations (3.9) and (3.10) look fully uncoupled and independent. However, the internal finite element forces $\mathbf{F}^{\mathrm{int}}$ are evaluated using the stresses within the fluid. The stresses, on the other hand, can be calculated from the interaction forces among particles, using the Irving-Kirkwood model [29], [30]

$$\boldsymbol{\sigma} = -n \left\langle \left[\sum_i m_i \hat{\mathbf{v}}_i \otimes \hat{\mathbf{v}}_i + \frac{1}{2} \sum_i \sum_{j \neq i} \mathbf{r}_{ij} \otimes \mathbf{f}_{ij} \right] \right\rangle \tag{3.12}$$

where n is the number density of particles; m_i is the particle mass; the vector $\hat{\mathbf{v}}_i$ is defined as $\hat{\mathbf{v}}_i = \mathbf{v}_i - \overline{\mathbf{v}}(\mathbf{x})$; $\overline{\mathbf{v}}(\mathbf{x})$ is the stream velocity at the position $\mathbf{x}$; $\mathbf{r}_{ij} = \mathbf{r}_i - \mathbf{r}_j$; and $\langle \ldots \rangle$ denotes the ensemble average. Therefore, the following functional relationship can be written:

$$\mathbf{F}^{\text{int}} = \mathbf{F}^{\text{int}}\left(\mathbf{f}^{\text{int}}\right) \tag{3.13}$$

This leads to the result that the differential equations of motion (3.9) and (3.10) are coupled through the force terms.

Instead to evaluate the forces $\mathbf{f}'^{ext}$ and $\mathbf{f}'^{\text{int}}$ and then calculate the fluctuation velocities $\mathbf{v}'$ from (3.9), it is more efficient to determine the forces $\mathbf{f}^{ext}$ and $\mathbf{f}^{\text{int}}$, use them to find the stresses within the fluid from (3.12), and then determine the nodal forces of the finite element needed in (3.10).

In order to couple the finite element balance equations and the mesoscale model, we write the finite element incremental-iterative equation for balance of linear momentum as:

$$\begin{bmatrix} \frac{1}{\Delta t}\mathbf{M} + {}^{n+1}\tilde{\mathbf{K}}^{(i-1)} & \mathbf{K}_{vp} \\ \mathbf{K}_{vp}^{T} & \mathbf{0} \end{bmatrix} \begin{Bmatrix} \Delta\mathbf{V}^{(i)} \\ \Delta\mathbf{P}^{(i)} \end{Bmatrix} =$$
$$\begin{Bmatrix} {}^{n+1}\mathbf{F}^{\text{int}(i-1)} \\ 0 \end{Bmatrix} + \begin{Bmatrix} {}^{n+1}\mathbf{F}_{ext}^{(i-1)} \\ 0 \end{Bmatrix} - \begin{bmatrix} \frac{1}{\Delta t}\mathbf{M} + {}^{n+1}\hat{\mathbf{K}}^{(i-1)} & \mathbf{K}_{vp} \\ \mathbf{K}_{vp}^{T} & 0 \end{bmatrix} \begin{Bmatrix} {}^{n+1}\mathbf{V}^{(i-1)} \\ {}^{n+1}\mathbf{P}^{(i-1)} \end{Bmatrix} + \begin{Bmatrix} \frac{1}{\Delta t}\mathbf{M}\,{}^{n}\mathbf{V} \\ 0 \end{Bmatrix} \tag{3.14}$$

where $\mathbf{V}$ and $\mathbf{P}$ are the nodal vectors of velocity and pressure; the matrices are defined in a usual manner [9]; $\mathbf{F}_{ext}$ is the external force; the upper left indices 'n' and 'n+1' denote the start and end of time step, and the right upper indices 'i-1' and 'i' are used for counting equilibrium iterations. The internal nodal force vector is:

$${}^{n+1}F_{Ki}^{\text{int}(i-1)} = -\int_{V} N_{K,j}\,{}^{n+1}\tau_{ij}^{(i-1)}\,dV \tag{3.15}$$

where ${}^{n+1}\tau_{ij}^{(i-1)}$ are the viscous stresses at end of time step, evaluated from the interaction DPD forces.

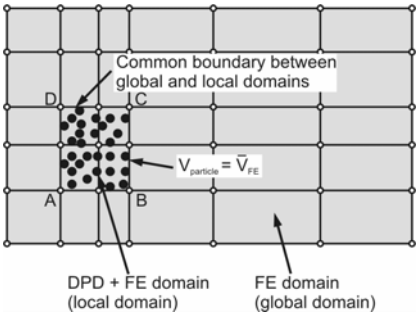

Figure 4 Two domains within a flow field: local domain - modeled by both DPD and FE methods; global domain modeled by FE method only. Boundary conditions at the common boundary between the local and global domains (velocities of particles are equal to those calculated using the FE model).

Finally, in order to achieve the main goals of this multiscale coupling specified in Section 3.1, we divide the entire fluid domain into the local domain (one or more), where the both mesoscopic (DPD) and continuum (FE) models are used, and

global domain discretized by continuum (FE) method only. A schematic representation of this division is shown in Fig. 4.

In order to calculate the flow field, it is necessary to satisfy the boundary conditions. External boundary are imposed on the coarse scale, i.e. the velocities or the stresses can be prescribed and used in the FE model. However, the boundary conditions at the common boundary between the local and global domains must also be specified. As shown in Fig. 4, for the DPD model we use the particle velocities at the common boundary to be equal to the coarse scale FE velocities. Also, the periodic boundary conditions are imposed on the common boundary to keep the number of particles constant. Various approaches in implementation of the periodic boundary conditions can be found elsewhere (e.g. [17], [19], [20],[31]).

In one example we illustrate application of the MBS method (other examples are given in [22]).

4 SMOOTHED PARTICLE HYDRODYNAMICS (SPH)

4.1 Introduction to the SPH method.

The smoothed particle hydrodynamics (SPH) is the also truly discrete particle method as the MD and DPD described in the previous sections. The basic idea in the SPH is representation of a physical field within a continuum by values at discrete points, considered as discrete material particles, using the so-called kernel approximation function. Then the continuum-based partial differential equations of balance are transformed into discrete particle equations. These discrete balance equations do not require space integration and use of a space mesh. The original version of SPH was developed for the modeling compressible fluid flows in astrophysical problems [32], [33]. Nowadays, applications of this Lagrangian method range from compressible/incompressible fluid flows to the structural mechanics.

We here present the fundamental equations of the SPH and show example solution of a simple flow of incompressible fluid. The main advantage of this method is that it does not require any mesh, while the shortcoming is a complexity of implementation of boundary conditions.

4.2 The basic equations of the SPH method.

The fundamental concept of the SPH is expressed by the relation

$$\langle f(\mathbf{r})\rangle = \int_V f(\mathbf{r}')W\left(|\mathbf{r}-\mathbf{r}'|,h\right)dV \tag{4.1}$$

Here $\langle f(\mathbf{r})\rangle$ is the kernel approximation of a function at a space point defined by the position vector $\mathbf{r}$; $W\left(|\mathbf{r}-\mathbf{r}'|,h\right)$ is called the *smoothing kernel function* or just *kernel* in SPH literature [34], [35], while h defines the size of the kernel support domain with the spatial volume V; and $\mathbf{r}'$ is the position vector of a point within the spatial domain. The SPH kernels have the 'compact support', which means that their value is equal to zero outside the support domain around **r.**

$$W\left(\left|\mathbf{r}-\mathbf{r}'\right|,h\right)=0 \quad \text{for} \quad \left|\mathbf{r}-\mathbf{r}'\right|\geq 2h \tag{4.2}$$

The kernel has to be normalized, i.e. it has to satisfy the condition:

$$\int_V W\left(\left|\mathbf{r}-\mathbf{r}'\right|,h\right)dV=1 \tag{4.3}$$

The above requirements ensure that kernel is approaching Dirac's delta function when h tends to zero, and the approximation of the function tends to the exact value:

$$\lim_{h\to 0} W\left(\left|\mathbf{r}-\mathbf{r}'\right|,h\right)=\delta\left(\left|\mathbf{r}-\mathbf{r}'\right|\right) \quad \text{and} \quad \lim_{h\to 0}\left\langle f(\mathbf{r})\right\rangle = f(\mathbf{r}) \tag{4.4}$$

When the function $f(\mathbf{r})$ is only known at a set of the discrete points, the integral equation (4.1) becomes the sum, and we have for $\mathbf{r}=\mathbf{r}^i$:

$$\left\langle f(\mathbf{r}^i)\right\rangle \equiv f\left(\mathbf{r}^i\right)\equiv f^i=\sum_{j=1}^{N}\frac{m^j}{\rho^j}f^j W^{ij} \tag{4.5}$$

where $f^j\equiv f(\mathbf{r}^j)$, $W^{ij}=W\left(\left|\mathbf{r}^i-\mathbf{r}^j\right|,h\right)$. Also, $m^j/\rho^j=\Delta V^j$ is the volume associated to particle j, and N is the number of particles within the support domain h. The term 'particle' in SPH has the same meaning as in the DPD method: the particle replaces its surrounding material and mass of the particle is constant during motion. A schematics of equation (4.5) is shown in Fig. 5.

In order to express the balance equations which have the form of partial differential equations [9], it is necessary to derive the expression for partial derivatives or gradient of a function with respect to space coordinates $x_\alpha, \alpha=1,2,3$. Following the basic approximation (4.11) we have that:

$$\left\langle \frac{\partial f(\mathbf{r})}{\partial x_\alpha}\right\rangle = \int_V W\left(\left|\mathbf{r}-\mathbf{r}'\right|,h\right)\frac{\partial f(\mathbf{r}')}{\partial x'_\alpha}dV \tag{4.6}$$

and integrating by parts finally follows:

$$\frac{\partial f^i}{\partial x_\alpha}=\sum_{j=1}^{N}\frac{m^j}{\rho^j}f^j\frac{\partial W^{ij}}{\partial x^i_\alpha} \tag{4.7}$$

Details of this derivation are given in [9]. Although the derivation of this expression is done correctly, an empirical relation for the derivatives is recommended [36]:

$$\frac{\partial f}{\partial x_\alpha}=\frac{1}{\rho}\left[\frac{\partial}{\partial x_\alpha}(\rho f)-f\frac{\partial \rho}{\partial x_\alpha}\right] \tag{4.8}$$

Next, we list two kernel functions. The most common is the B-spline function [37]:

$$W(\nu,h)=\frac{C}{h^D}\begin{cases}\left(1-\frac{3}{2}\nu^2+\frac{3}{4}\nu^3\right) & \nu<1\\ \frac{1}{4}(2-\nu)^3 & 1\le\nu\le 2\ ;\ \nu=\left|\mathbf{r}-\mathbf{r}'\right|/h\\ 0 & \nu>2\end{cases} \tag{4.9}$$

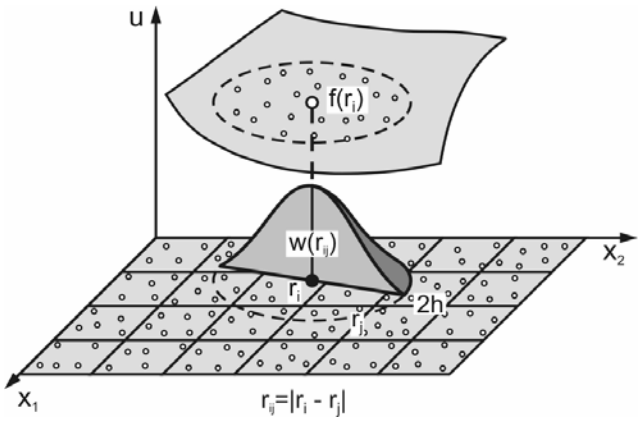

Figure 5 A schematics of the SPH interpolation. Value of function *f* at a discrete point '*i*' is interpolated from the values of surrounding points within the support domain of radius 2*h* by use of the kernel function $W(r_{ij})$.

where *D* is the number of the dimensions of the problem (1, 2 or 3). The constant *C* is the scaling factor which has to provide that equations (4.2) and (4.3) are satisfied: C=2/3, $C=10/(7\pi)$, $C=1/\pi$ for D=1, 2, 3, respectively. The second is a quintic spline, which for 2D problems is:

$$W(\nu,h)=\frac{7}{478\pi}\begin{cases}(3-\nu)^5-6(2-\nu)^5+15(1-\nu)^5 & 0\le\nu<1\\ (3-\nu)^5-6(2-\nu)^5 & 1\le\nu<2\ ;\ \nu=\left|\mathbf{r}-\mathbf{r}'\right|/h\\ (3-\nu)^5 & 2\le\nu<3\\ 0 & \nu\ge 3\end{cases} \tag{4.10}$$

The usage of quintic kernel approximately doubles the computational time, but gives more stable results.

Finally, we give the SPH equations of balance of mass (continuity equation) and

balance of linear momentum. They are:

$$\frac{d\rho^i}{dt} = \sum_{j=1}^{N} m^j (v_\beta^i - v_\beta^j) \frac{\partial W^{ij}}{\partial x_\beta^i}$$

$$\frac{dv_\alpha^i}{dt} = \sum_{j=1}^{N} m^j \left[\left(\frac{\sigma_{\alpha\beta}^j}{\left(\rho^j\right)^2} + \frac{\sigma_{\alpha\beta}^i}{\left(\rho^i\right)^2} \right) \frac{\partial W^{ij}}{\partial x_\beta^i} + \frac{f_\alpha^{Vj}}{\rho^j} W^{ij} \right] \quad \begin{array}{l} \text{sum on } \beta: \ \beta = 1,2,3 \\ \text{no sum on } i \end{array} \qquad (4.11)$$

Details of derivation of these equations are given in [9].

5 ELEMENT-FREE GALERKIN (EFG) METHOD

5.1 Introduction to the EFG method

The so-called element-free Galerkin (EFG) method can be considered as a computational procedure which overcomes the shortcomings of the mentioned methods. The fundamental idea of the EFG method is to represent the field of a physical quantity by values at a set of discrete points which are not associated with a mesh as in the FE method, i.e. the points are element-free. These points are usually called the free points. The approximate value of a quantity at material point within the domain is obtained by use of the weight-type interpolation functions within a domain of influence. The weight functions decay with the distance from the material point and are negligible outside the domain of influence, as schematically shown in Fig. 6a.

Finally, note that the EFG is in essence a continuum method. Discretization of the continuum leads to discrete (free) points, but evaluation of the matrices and vectors within the discrete balance equations is performed over the continuous subdomain

5.2 Formulation of the EFG method

The interpolated value $u(\mathbf{r})$ of a physical quantity (spatial function) at a point, which we call the material point, with the position vector $\mathbf{r}$, is given as [38]:

$$u(\mathbf{r}) = \sum_{j}^{m} p_j(\mathbf{r}) a_j(\mathbf{r}) \equiv \mathbf{p}^T(\mathbf{r}) \mathbf{a}(\mathbf{r}) \qquad (5.1)$$

where $p_j(\mathbf{r})$ are the components of the base vector $\mathbf{p}(\mathbf{r})$, expressed as monomials in the coordinates of $\mathbf{r}[x, y, z]$ so that the basis is complete; the component $p_1 = 1$; and m is the basis size. The coefficients $a_j(\mathbf{r})$ are to be determined. The linear and quadratic bases for one-dimensional space are:

$$\mathbf{p}^T(\mathbf{r}) = [1, x], \ \text{linear}, \ m = 2; \quad \mathbf{p}^T(\mathbf{r}) = \left[1, x, x^2\right] \ \text{quadratic, m=3} \qquad (5.2)$$

These bases for the 2D space are:

$$\mathbf{p}^T(\mathbf{r}) = [1, x, y]; \qquad \text{linear,} \qquad m = 3; \tag{5.3}$$

$$\mathbf{p}^T(\mathbf{r}) = \left[1, x, y, x^2, xy, y^2\right], \quad \text{quadratic,} \quad m=6 \tag{5.4}$$

The coefficients $a_j(\mathbf{r})$ are functions of the position vector and are determined by minimizing a weighted quadratic form:

$$J = \sum_{K=1}^{n} w\left(\mathbf{r} - \mathbf{r}^K\right)\left[\mathbf{p}^T\left(\mathbf{r}^K\right)\mathbf{a}(\mathbf{r}) - U^K\right]^2 \tag{5.4}$$

where K denotes the free point number with the position vectors $\mathbf{r}^K$ and with the value of the function U^K; $w\left(\mathbf{r} - \mathbf{r}^K\right)$ is the weight function which depends on the distance between the material point and free point; and n is the number of free points in the domain of influence around the material point. Minimizing J with respect to the coefficients $a_j(\mathbf{r})$, the system of equations is obtained:

$$\frac{\partial J}{\partial a_i} = 2\sum_{K=1}^{n} w^K\left(p_j^K a_j - U^K\right)p_i^K = 0 \text{ , sum on } j\text{: } j = 1,2,...,m \tag{5.5}$$

where $w^K \equiv w\left(\mathbf{r} - \mathbf{r}^K\right)$, $p_j^K \equiv p_j\left(\mathbf{r}^K\right)$. Note that w^K also depends on the position vector $\mathbf{r}$ of the material point. This system of equations can be written in the form:

$$A_{ij}a_j - B_{iK}U^K = 0, \qquad \text{sum on } K \text{ and } j : K = 1,2,...,n; j = 1,2,...,m \tag{5.6}$$

where the matrices $\mathbf{A}$ and $\mathbf{B}$ are:

$$A_{ij} = \sum_{I=1}^{n} w^I p_i^I p_j^I; \qquad B_{iK} = p_i^K w^K, \quad \text{no sum on } K \tag{5.7}$$

The matrices $\mathbf{A}$ and $\mathbf{B}$ are of order $m \times m$ and $m \times n$, respectively. Equation (5.6) can be solved for the coefficients $a_j(\mathbf{r})$, hence.

$$\mathbf{a}(\mathbf{r}) = \mathbf{A}^{-1}\mathbf{B}\mathbf{U}; \qquad \text{or} \qquad a_j(\mathbf{r}) = \sum_{K=1}^{n}\left(\mathbf{A}^{-1}\mathbf{B}\right)_{jK} U^K \tag{5.8}$$

Now, substitution of $\mathbf{a}(\mathbf{r})$ from (5.8) results into (5.1) follows:

$$u(\mathbf{r}) = \mathbf{p}^T\mathbf{A}^{-1}\mathbf{B}\mathbf{U} = \sum_{K=1}^{n}\Phi_K(\mathbf{r})U^K \tag{5.9}$$

the interpolation function $\Phi_K(\mathbf{r})$ corresponding to the free point K, is:

$$\Phi_K(\mathbf{r}) = \sum_{j=1}^{m}\left(\mathbf{A}^{-1}\mathbf{B}\right)_{jK} p_j \tag{5.10}$$

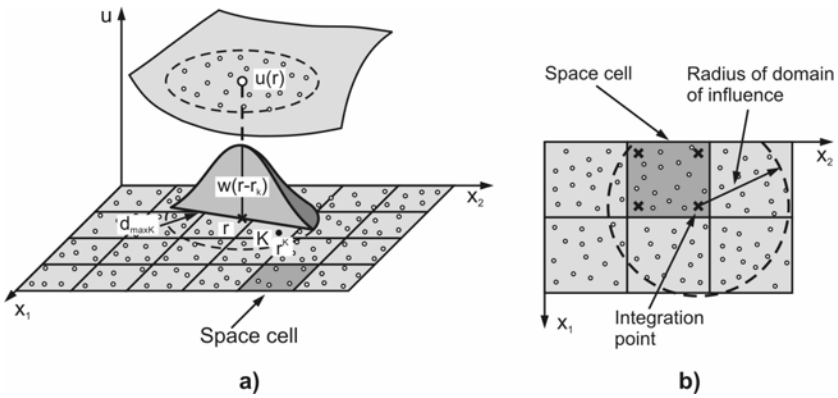

Figure 6 Interpolation by EFG method (2D domain). **a)** Function $u(\mathbf{r})$ at a material point with the position vector **r**. The weight functions $w(\mathbf{r}-\mathbf{r}^K)$ decreases with the distance between the material point and the free points *K*; $d_{\max K}$ defines the size of the domain of influence for the weight function $w(\mathbf{r}-\mathbf{r}^K)$; **b)** Space cell used for integration and domain of influence around the integration point.

The form (5.9) is the same as in the FE method. Here, the interpolation functions are expressed in terms of the Cartesian coordinates x_i and x_i^K of the material and free point, while in the FE method they are expressed in terms of the natural coordinates of a finite element [1]-[9].

It is necessary in applications to calculate the derivatives with respect to the coordinates x_i. From (5.10) follows:

$$\Phi_{K,i}=\sum_{j=1}^{m}\left[\left(\mathbf{A}^{-1}\mathbf{B}\right)_{jK}p_{j,i}+\left(\mathbf{A}^{-1}_{,i}\mathbf{B}+\mathbf{A}^{-1}\mathbf{B}_{,i}\right)_{jK}p_j\right] \tag{5.11}$$

where $_{,i}\equiv\partial/\partial x_i$. By differentiation of the equation $\mathbf{A}^{-1}\mathbf{A}=\mathbf{I}$ we obtain:

$$\mathbf{A}^{-1}_{,i}=-\mathbf{A}^{-1}\mathbf{A}_{,i}\mathbf{A}^{-1} \tag{5.12}$$

which can be used to evaluate $\mathbf{A}^{-1}_{,i}$.

We further give one of the weight functions, of the exponential form [38]:

$$w^I\left(d_I^{2k}\right)=\begin{cases}\dfrac{\exp\left(-d_I/c\right)^{2k}-\exp\left(-d_{\max I}/c\right)^{2k}}{1-\exp\left(-d_{\max I}/c\right)^{2k}}, & d_I\le d_{\max I}\\ 0, & d_I\le d_{\max I}\end{cases} \tag{5.13}$$

where $d_I=\left\|\mathbf{r}-\mathbf{r}^I\right\|$ is the distance between the material point and the free point *I*; $d_{\max I}$ is the domain of influence for the weight function w^I; *k* is the parameter (in our

applications we use $k=1$); and:

$$c=\alpha \max\left\|\mathbf{r}_K-\mathbf{r}_J\right\| \qquad \text{for all free points} \tag{5.14}$$

where $1\le\alpha\le 2$ is recommended. Another form of the weight function and graphical representations are given in [9].

Once the interpolation functions are formulated, the procedure is computationally similar to that of the FE method. For an integration point, shown in Fig. 6b, the 'element' nodes include all free points within the domain of influence. Of course, the FE interpolation functions N_K are now replaced by the EFG interpolation functions Φ_K.

We perform integration over selected volumes as the subdomains (Figs. 6a,b) of the physical field to form the balance equations for the entire domain. In this case the subdomains are called volume cells and are defined independently of the free points. We simply integrate over the volume cells numerically by, say, Gauss quadrature, and add contributions to the matrices and vectors corresponding to variables at free points (degrees of freedom of free points) within the domain of influence, see Fig. 6b. The independence of volume cells on the free points is the main advantage of the EFG method. To increase solution accuracy, number of integration points within a cell can be adjusted to the number of free points [38], [39].

The EFG model can be coupled with a FE model. Details about this coupling are given in [9] and [39].

In one example we illustrate the robustness and accuracy of the EFG method.

6 EXAMPLES

We here give two typical examples which illustrate application of the discrete particle methods described above.

6.1. Unsteady flow between two plates.

We consider flow of incompressible fluid between two stationary infinite plates located at y=0 and y=H. The fluid is initially at rest and it is driven by body force (given here as acceleration a) parallel to x axis. The analytical solution ($v\equiv v_x$) is given as a series [40]:

$$v(y,t)=\frac{a}{2\nu}y(y-H)+ \\ +\sum_{n=0}^{\infty}\frac{4aH^2}{\nu\pi^3(2n+1)^3}\sin\left(\frac{\pi y}{H}(2n+1)\right)\exp\left(-\frac{(2n+1)^2\pi^2\nu}{H^2}t\right)$$

Parameters used in SPH model are: kinematic viscosity $\nu=10^{-6}m^2s^{-1}$, fluid density $\rho=10^3kgm^{-3}$, $H=10^{-3}m$, $a=10^{-4}ms^{-2}$, $\Delta t=10^{-4}$s and 30 particles spanning the space between plates.

Velocity profiles for several times are shown in Fig. 7. It can be seen very good agreement between the solutions obtained using DPD, EFG and SPH methods and analytical solutions. We also give the finite element solution (FE) which is practically the same as the solutions obtained by the discrete particle methods.

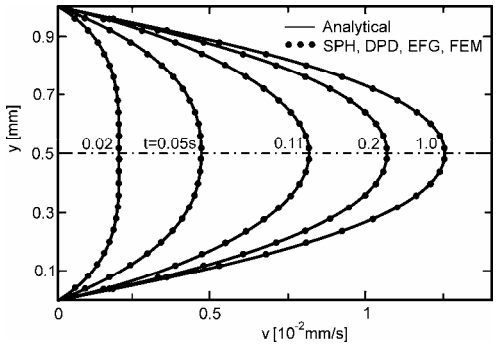

Figure 7 . Velocity profiles for several times. Analytical and numerical solutions (methods: SPH- smoothed particle hydrodynamics; DPD – dissipative particle dynamics; EFG – element free Galerkin; FEM – finite element.

6.2. Fluid flow in a microchannel with narrowing.

We here consider a steady fluid flow between two parallel plates with narrowing, Fig. 8a. We solve this example using the DPD and SPH, as well as the multiscale (DPD+FE) method to demonstrate applicability of these methods to modeling of microcirculation.

Parameters used in the DPD and SPH models are the same as in Example 6.1 (see also data in the figure caption). For the comparison, the finite element (FE) solution is shown.

In the FE-DPD multiscale MBS model (Section 3) the local DPD+FE domain, as well as the global FE domain, are shown in Fig. 8b. At the common boundary between the local and global domains the mesoscale DPD particle velocities are equal to the coarse scale FE velocities. The periodic boundary conditions are imposed at the common boundary to keep the number of particles constant.

Velocity profiles are shown in Fig. 8c, where a significant velocity increase in the domain of narrowing (stenosis) is notable. The solutions using the DPD, SPH and FE-DPD multiscale MBS methods compare well with the FE solution.

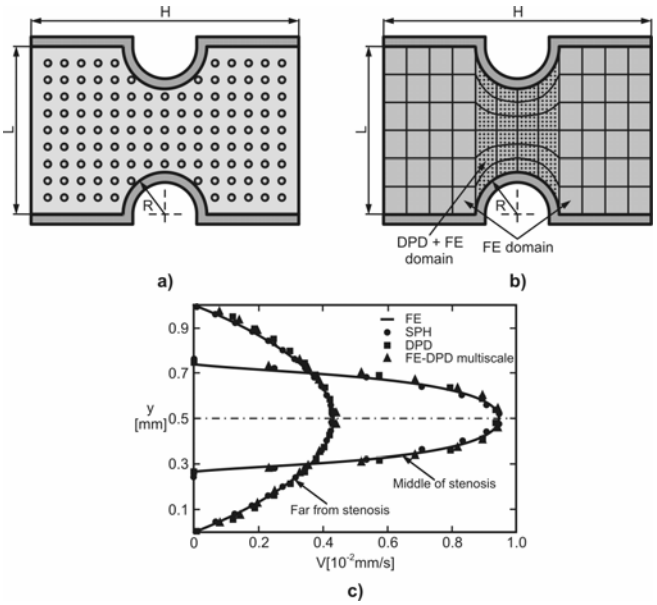

Figure 8 Steady blood flow in a channel with narrowing. **a)** Geometry of the channel and SPH initial particle positions, **b)** Local (DPD+FE) and global (FE only) domains used for the multiscale MBS method; **c)** Velocity profiles (FE, DPD, SPH and DPD-FE multiscale solutions). Data: kinematic viscosity $v=10^{-6}[m^2s^{-1}]$, fluid density $\rho=10^{3}[kgm^{-3}]$, $H=10^{-3}[m]$, acceleration $a=10^{-3}[ms^{-2}]$, pressure gradient.

7 SUMMARY AND CONCLUSIONS

A review of some of the discrete particle methods is presented. We have selected the methods which are currently of interest for general applications. These methods are still in a developing stage and their further refinements and improvements may be expected.

The discrete particle methods have the features which overcome deficiencies of the finite element method, which can be summarized as:

a) The methods are mesh-free, therefore there is no need for remeshing when the computational domain changes significantly during the analysis. The remeshing is very complex computational procedure in a general geometrical conditions and is very demanding with respect to the computer resources as well as in the computing efforts.

b) The discrete particle methods can be applied to complex problems where the FE method practically cannot be employed (e.g. flow of colloidal fluids).

However, the discrete particle methods have serious drawbacks:

a) The methods demand huge models, with enormous number of equations

which can be measured in millions; this is particularly true for 3D conditions;

b) The methods are very complex to be used in general 3D analyses. Here, the EFG has the advantage with respect to other discrete-type methods, since it can be coupled in a straightforward manner to the FE method [38], [39];

c) Implementation of the boundary conditions are in general very complicated to be easily used and still are not developed for general conditions [17]-[20];

d) A multiscale MBS method [21], [22] offers a possibility to couple a discrete mesoscale particle method, such as the DPD method, to a continuum-based methods (FE, EFG), but further research is needed to establish necessary relations for general applications.

ACKNOWLEDGMENTS

This study is partly supported by Ministry of Science and Environmental Protection of Serbia, projects TR12007 and OI144028, and City of Kragujevac.

REFERENCES

[1] Huebner, K. H. (1975): The Finite Element method for Engineers, J. Wiley and Sons, New York.

[2] Sekulovic, M. (1984): The finite Element Method, (in Serbian), Gradjevinska knjiga, Belgrade, Serbia.

[3] Hughes, T. J. R. (1987): The Finite Element Method. Linear Static and Dynamic Finite Element Analysis, Prentice Hall, Inc., Englewood Cliffs, N.J.

[4] Crisfield, M. A. (1991): Non-Linear Finite Element Analysis of Solids and Structures, J. Wiley & Sons, Chichester, England.

[5] Bathe, K. J. (1996): Finite Element Procedures, Prentice-Hall, Englewood Cliffs, N. J.

[6] Kojic, M., Slavkovic, R., Zivkovic, M., Grujovic, N. (1998): The Finite Element method – Linear Analysis, (in Serbian), Faculty of Mech. Eng., Univ. Kragujevac, Serbia.

[7] Kojic, M. and Bathe K. J. (2005): Inelastic Analysis of Solids and Structures, Springer, Berlin – Heidelberg.

[9] Kojic M., Filipovic N., Stojanovic, B.and Kojic, N. (2008): Computer Modeling in Bioengineering – Theoretical Background, Examples and Software, J. Wiley and Sons, Chichester, England.

[10] Gerstein, M., Levitt, M. (2005): Simulating water and the molecules of life, Scientific American (The Water of Life, Special Issue), pp. 24-29.

[11] Curtin, W. A. and Miller, R. E. (2003): Atomistic/continuum coupling in computational material science, Mod. Simul. Mater. Sci. Engrg., Vol. 11, pp. 33-68.

[12] Flekkoy, E. G., Coveney, P. V. and De Fabritiis, G. (2000): Foundations of dissipative particle dynamics, Phys. Rev. E, Vol. 62, pp. 2140-2157.

[13] Serrano, M., De Fabritiis, G., Espanol, P., Flekoy, E. G. and Coveney, P. V. (2002): Mesoscopic dynamics of Voronoy fluid particles, J. Physics A, Vol. 35,

pp. 1605-1625.
[14] Hoogerbrugge, P. J. and Koelman J. M. V. A. (1992): Simulating microscopic hydrodynamic phenomena with dissipative particle dynamics, Europhys. Lett., Vol. 19, pp. 155-160.
[15] Espanol, P. and Warren P. (1995): Statistical mechanics of dissipative particle dynamics, Europhys. Lett., Vol.30, Issue 4, pp. 191-196.
[16] Groot, R. D. and Warren, P. B. (1997): Dissipative particle dynamics: Bridging the gap between atomistic and mesoscopic simulation, J. Chem. Phys., Vol. 107, Issue 11, pp. 4423-4435.
[17] Haber, S., Filipovic, N., Kojic, M. and Tsuda, A. (2006): Dissipative particle dynamics simulation of flow generated by two rotating concentric cylinders, Phys. Rev. E., Vol. 74, pp. 1-8.
[18] Koplik, J. and Banavar, J. R. (1995): Corner flow in the sliding plate problem, Phys. Fluids, Vol. 7, Issue 12, pp. 3118–3125.
[19] Pivkin, I. and Karniadakis, G. E. (2005): A new method to impose no-slip boundary conditions in dissipative particle dynamics, J. Comp. Phys., Vol. 207, pp. 114-128.
[20] Filipovic N., Ravnic, D., Kojic, M., Mentzer, S. J., Haber, S. and Tsuda A. (2008): Platelet adhesion to a collagen wall: Experimental investigation and computer modeling by Discrete Particle Dynamics Method, Microvascular Research, in press.
[21] Kojic, M., Filipovic, N. and Tsuda, A. (2006): A multiscale method for bridging dissipative particle dynamics and Navier-Stokes finite element equations for incompressible fluid and its application in biomechanics, Proc. First South-East European Conference on Comp. Mechanics (Eds. M. Kojic and M. Papadrakakis), Kragujevac, Serbia, 28-30 June, pp. 345-350.
[22] Kojic, M., Filipovic, N. and Tsuda, A (2008): A mesoscopic bridging scale method for fluids and coupling dissipative particle dynamics with continuum finite element method, Comp. Meth. Appl. Mech. Eng., in press.
[23] Curtin, W. A. and Miller, R. E. (2003): Atomistic/continuum coupling in computational material science, Mod. Simul. Mater. Sci. Eng. , Vol. 11, pp. R33-R68.
[24] Liu, W. K., Karpov, E. G., Zhang, S. and Park, H. S. (2004): An introduction to computational nanomechanics and materials, Comput. Meth. Appl. Mech. Engrg., Vol. 193, pp. 1529-1578.
[25] Liu, W. K., Qian, D. and Horstemeyer, M. F. (2004): Preface, Comput. Meth. Appl. Mech. Engrg., Special Issue, Vol. 193, pp. iii-iv.
[26] Nielsen, S. O., Lopez, C. F., Srinivas, G. and Klein, M. L. (2004): Coarse grain models and computer simulation of soft materials, J. Physics: Condens. Matter., Vol. 16, pp. R481-R512.
[27] Wagner, G. J. and Liu, W. K. (2003): Coupling of atomistic and continuum simulations using a bridging scale decomposition, J. Comput. Physics, Vol. 190, pp. 249-274.
[28] Tang, S., Hou, T. H. and Liu, W.K. (2006): A mathematical framework of the bridging scale Method, Int. J. Num. Meth. Eng., Vol. 65, pp. 1688-1713.
[29] Fan, X., Phan-Thien, N., Yong, N. T., Wu, X. and Xu, D. (2003): Microchannel

flow of a macromolecular suspension, Physics of Fluids, Vo. 15, pp. 11-21.
[30] Ren, W. and E, W. (2005): Heterogeneous multiscale method for the modeling of complex fluids and micro-fluidics, J. Comp. Phys., Vol. 204, pp. 1-26.
[31] Revenga, M., Zuniga, I., Espanol. P. and Pagonabarraga, I. (1998): Boundary models in DPD, Int. J. Mod. Phys. C, Vol. 9, pp. 1319-1331.
[32] Ginhold, R. A. and Monaghan, J. J. (1977): Smoothed Particle Hydrodynamics: Theory and application to non-spherical stars, Mon. Not. R. Astron. Soc., Vol. 181, pp. 375-389.
[33] Lucy, L. B. (1977): A numerical approach to the testing of fusion process, Astronomical J., Vol. 88, pp. 1013-1024.
[34] Belytschko, T., Krongauz, Y., Organ, D., Fleming, M. and Krysl, P. (1996): Meshless Methods: An overview and recent developments, Comp. Meth. Appl. Mech. Engrg, Vol. 139, pp. 3-47.
[35] Vignjevic R. (2004): Review of development of the smooth particle hydrodynamics (SPH) method, Dynamics and Control of Systems and Structures in Space (DCSSS), 6th Conference, Riomaggiore, Italy.
[36] Monaghan, J. J. (1994): Simulating free surface flows with SPH, J. Comput. Phys., Vol. 110, pp. 399-406.
[37] Monaghan, J. J. and Gingold, R. A. (1983): Shock simulation by the particle method SPH, J. Comp. Phys., Vol. 52, pp. 374-389.
[38] Belytschko, T., Lu, Y. Y. and Gu, L. (1994): Element-free Galerkin methods, Int. J. Num. Meth. Engrg., Vol. 37, pp. 229-256.
[39] Vlastelica, I. (2003): Methods of Solving Elastoplastic Deformation of Non-Porous and Porous Metals in Fracture Mechanics, Ph.D. thesis (in Serbian), Faculty of Mech. Eng., Univesity of Kragujevac, Serbia.
[40] Morris, P. J., Fox J. P. and Zhu, Y. (1997): Modeling Low Reynolds Number Incompressible Flows Using SPH, J. Comp. Phys., Vol. 136, pp. 214-226.

Sent: Friday, April 11, 2008, 3:24 PM